Astron. Astrophys. 319, 235–243 (1997)

ASTRONOMY AND ASTROPHYSICS

A survey of CN in circumstellar envelopes⋆

R. Bachiller[1], **A. Fuente**[1], **V. Bujarrabal**[1], **F. Colomer**[1], **C. Loup**[2], **A. Omont**[2], **and T. de Jong**[3]

[1] Observatorio Astronómico Nacional (IGN), Apartado 1143, E-28800 Alcalá de Henares, Madrid, Spain
[2] Institut d'Astrophysique de Paris (CNRS), 98 bis Bd. Arago, F-75014 Paris, France
[3] SRON, Space Research Groningen, P.O. Box 800, 9700 AV Groningen, The Netherlands

Received 15 April 1996 / Accepted 22 July 1996

Abstract. We have conducted a survey of CN N=2–1 and N=1–0 line emission in the envelopes of evolved stars. The sample consists of 42 objects, including C-rich and O-rich envelopes, S-stars, detached envelopes, and proto-planetary nebulae. Confident detections have been achieved in 30 objects. Both CN lines are bright in C-rich envelopes, and the 2–1 line has been detected in 5 O-rich objects (previously, CN had been detected in only one O-rich envelope). The excitation temperature $T_{\rm rot}$, evaluated from the 2–1/1–0 intensity ratio, is $\sim$ 3–6 K in most carbon stars, and $\geq$ 10–20 K in O-rich envelopes.

We find that the CN spectra display anomalies in the rotational, fine, and hyperfine line ratios. Anomalies in the rotational excitation appear in W Ori and UU Aur, two stars which are known to present HCN v=0 J=1–0 masers. The excitation of the CN 2–1 line is unusually high in both objects, and UU Aur may present a weak maser effect in this line. Anomalies are also observed in the intensity ratios of the fine and hyperfine components. If such anomalies were due to the envelope thickness, the required line opacities would be excessively high, in particular for low mass-loss rate objects. We thus suggest that the observed anomalies are the result of an anomalous excitation. Pumping through the optical and near-IR bands seems to play a dominant role in the CN excitation.

A comparison with previously published HCN data shows that the CN/HCN ratio of the total numbers of molecules in C-rich stars tends to be larger in the objects with lower mass-loss rate, supporting the idea that CN is mainly formed from the photodissociation of HCN. The average peak abundance of CN is $\sim 1.9\,10^{-5}$ in C-rich objects, and is about 300 times smaller ($\sim 6.6\,10^{-8}$) in O-rich envelopes. The CN/HCN peak abundance ratio is $\sim$0.45 in C-rich stars, in agreement with photodissociation chemical models, and $\sim$0.04 in O-rich objects. This last value is about two orders of magnitude smaller than the predictions of standard chemical models, and suggest that CN is destroyed by additional mechanisms than photodissociation in O-rich envelopes.

Key words: stars: circumstellar matter – stars: AGB, post-AGB – stars: abundances – radio lines: stars – molecular processes

1. Introduction

The copious mass loss undergone by stars on the asymptotic giant branch leads to the formation of circumstellar envelopes (CSEs). The low temperature of the central stars allows the production of many molecular species in gas phase within their atmospheres and envelopes. The chemistry of this circumstellar gas can be very rich, and depends on the value of the C/O ratio, the thickness of the envelope, and the ambient ultraviolet field (e.g. Omont 1985). Radio molecular spectroscopy is one of the most powerful tools to investigate the structure, kinematics, and chemical composition of CSEs; and extensive studies of the most abundant molecules such as CO, SiO, and HCN have provided important insights into the envelopes (e.g. Olofsson et al. 1993a,b, Bujarrabal et al. 1994, Loup et al. 1993, Nercessian et al. 1989).

The cyanogen radical (CN) is known to be one of the most abundant molecules in the CSEs of C-rich stars (i.e. stars in which C/O $>$ 1). In IRC+10216, the CN abundance is only a factor of $\sim$ 5 lower than that of HCN (Omont 1992, Dayal & Bieging 1995). In other CSEs, CN also has a high abundance (Olofsson et al. 1993b) and CN has been detected toward one O-rich envelope (TX Cam, Olofsson et al. 1991). On the other hand, chemical models predict that CN is the direct photodissociation product of HCN (Huggins & Glassgold 1982, Lafont et al. 1982, Huggins et al. 1984, Nejad & Millar 1987). Moreover, observations of CN and HCN toward evolved planetary nebulae (PNe) (Cox et al. 1993; Bachiller et al. 1996) indicate that the photodissociation of HCN during the proto-PN and PN phases results in an enhancement of CN with respect to HCN. It thus appears that the CN abundance and the CN/HCN abundance

Send offprint requests to: R. Bachiller

⋆ Tables 1 and 2 are only available in electronic form at the CDS via anonymous ftp to cdsarc.u-strasbg.fr (130.79.128.5) or via http://cdsweb.u-strasbg.fr/Abstract.html

ratio can vary significantly depending on the type of star and on the degree of evolution.

In order to determine the CN abundance, one needs to make assumptions on the molecule excitation, and radiative transfer models have been already developed (e.g. Truong-Bach et al. 1987). However, the CN excitation mechanisms in CSEs remain poorly understood, in particular because IR and possibly optical pumping is likely important in determining the population of the rotational ladders. Systematic multiline studies of CN in a variety of CSEs are needed to provide new pieces of information on its excitation and chemistry. In this paper, we present a high-sensitivity survey of CN in CSEs. The sample includes a large assortment of objects. Since we were interested in the molecular excitation, we simultaneously observed the two lowest rotation lines N=1–0 and 2–1. Each of these lines is split in several fine and hyperfine structure components (see below). In order to assess optical depths we observed all the 1–0 components, and the two main groups of the 2–1 line; the third group which was not observed only shares 6 % of the 2–1 emission.

2. Observations

The observations were carried out with the IRAM 30-m radio telescope at Pico Veleta (near Granada, Spain) in July 1990 and December 1994. In 1994, we used two SIS receivers operating in the bands around $\lambda\lambda$ 3 mm, and 1 mm to simultaneously observe the N=1–0 and 2–1 lines of CN. The SSB noise temperatures of the receivers were 140 K at 113.5 GHz, and 160 K at 226.8 GHz. The antenna half-power beamwidths (HPBW) and main beam efficiencies were $22''$ and 0.68 at 113 GHz, and $12''$ and 0.40 at 226 GHz. Pointing was checked every hour by observing nearby planets or continuum sources, and was found to be accurate to within $3''$. The spectrometers were filterbanks providing a spectral resolution of 2.64 km s^{-1} at 113 GHz, and 1.32 km s^{-1} at 226 GHz. In 1990, we used two receivers in the 3 mm band to observe the N=1–0 line of CN simultaneously with the J=1–0 line of HCN, and the 2–1 line of CN was not observed. The objects observed in both runs were found to have the same CN N=1–0 intensities within the observational uncertainties. All observations were made in position switching mode by wobbling the secondary mirror by 2– $4'$ in azimuth. The calibration of the data was achieved by the chopper wheel method. Linear baselines were subtracted from the spectra. Intensities are given in units of main beam brightness temperature. For completeness, we also discuss here some observations of CRL618, AFGL2688, and NGC7027 obtained by Bachiller et al. (1996).

3. Observational results: properties of the CN profiles

We list in Table 1 the observed stars together with some of their characteristics. Distances, expansion velocities, mass loss rates, and spectral types are taken from the compilations of Bujarrabal et al. (1994) and Loup et al. (1993). The sample includes C-rich and O-rich objects, some S-stars, a few proto-PN, and a young PN (NGC7027).

Some of the observed profiles are shown in Fig. 1 (C-rich envelopes), Fig. 2 (O-rich objects), and Fig. 3 (other stars). The profiles exhibit a quite complex structure which is due to the splitting of the CN rotational levels. In fact, the unpaired electron spin of CN, together with the nonzero spin of the nitrogen nucleus, splits each rotational line into many fine and hyperfine components with different intensities. The N=1–0 rotational transition near 113.3 GHz results in 9 HF components grouped in two main fine-structure groups; while the N=2–1 transition near 226.6 GHz is split in 18 HF lines which are grouped in three fine-structure packs. The profiles of Figs. 1, 2, and 3 contain all the 1–0 components (two groups), and the two main groups of the 2–1 line.

Bright CN emission is observed toward the C-rich objects, with peak intensities $\gtrsim$ 1 K measured in several of these CSEs. In addition, weak CN 2–1 emission has been detected toward 5 O-rich CSEs (IK Tau, TX Cam, VY CMa, NML Cyg, and IRC+10420), whereas the 1–0 line was tentatively detected toward NML Cyg and IRC+10420. The 2–1 intensity measured toward TX Cam is in good agreement with the previous measurements by Olofsson et al. (1991). The S-stars W Aql and χ Cyg exhibit relatively strong lines. Finally two C-rich PPNe (CRL618 and CRL2688) and the young PN NGC7027 present very bright emission lines. The emission is weaker toward the C-rich PPN SAO96709, a very distant ($d \sim 4$ kpc) object which also exhibits weak HCN emission (Omont et al. 1993). The profile shapes are flat-topped or parabolic in most objects, indicating that they are unresolved by the antenna beam. However, IRC+10216, S Cep, and RY Dra exhibit two-horn profiles characteristic of resolved envelopes (see Fig. 1).

In Table 2, we give some of the observational parameters. $A_{\rm low}$ and $A_{\rm high}$ refer to the integrated intensity of the low-frequency and high-frequency fine-structure groups. The intrinsic intensity ratios, R=$A_{\rm high}/A_{\rm low}$, are R(1–0) = 2 and R(2–1) = 1.8. In principle, the observation of several components with different intrinsic strengths allows an estimate of the line optical depth, and the value of R gives an estimate of the envelope thickness. It is noticeable that the observed values of R(1–0) and R(2–1) are smaller than the intrinsic values in most stars. Many objects exhibit values of R which are < 1. The mean values of R(1–0) and R(2–1) are 1.3 and 1.1, respectively, for C-rich stars. The average value of R(2–1) is 1.2 for the O-rich stars. The two O-rich objects tentatively detected in 1–0 emission, NML Cyg and IRC+10420, have R(1–0) = 1.2 and 1.5, respectively. Similar low values of R were also observed in the 1–0 line by Olofsson et al. (1993b) in a sample of 12 stars, 6 of which were not observed by us. At first sight, the most obvious explanation of such low values of R is that the lines are optically thick.

We tried to obtain the line opacities from the observed profiles. By assuming that the lines are optically thick, we made non-linear least square fits to the spectra with synthetic profiles consisting of a sum of n gaussians (where n is the number of the HF components) which are spaced in velocity following the HF structure, and which have the same linewidth. The parameters of the fit are: (i) the linewidth, (ii) the central velocity of the main

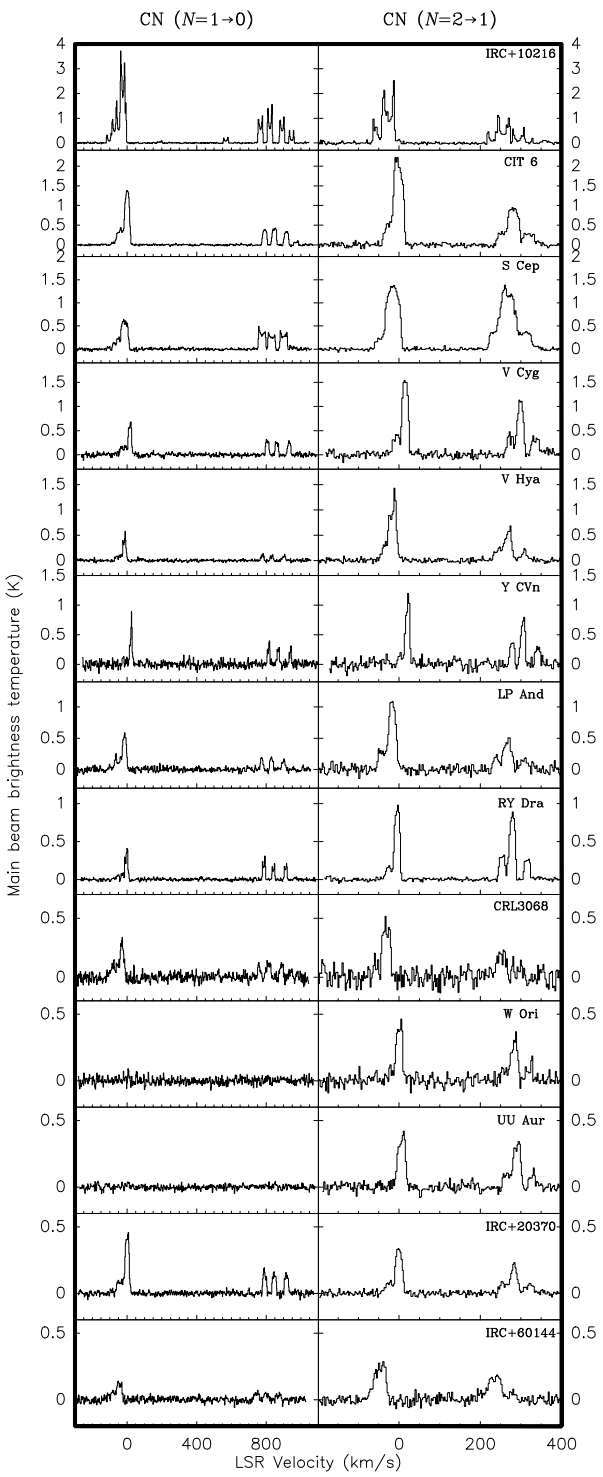

Fig. 1. Some of the CN profiles observed toward C-rich stars. The profiles consist of two fine-structure groups of hyperfine components. The velocity scales are calculated with respect to the frequency of the strongest component of both lines (N=1–0, J=3/2–1/2, F=5/2–3/2, 113.490945 GHz; and N=2–1, J=5/2–3/2, F=7/2–5/2, 226.874766 GHz). Note that W Ori and UU Aur exhibit a very high (N=2–1)/(N=1–0) intensity ratio. The N=2–1 line could be a weak maser at least in UU Aur.

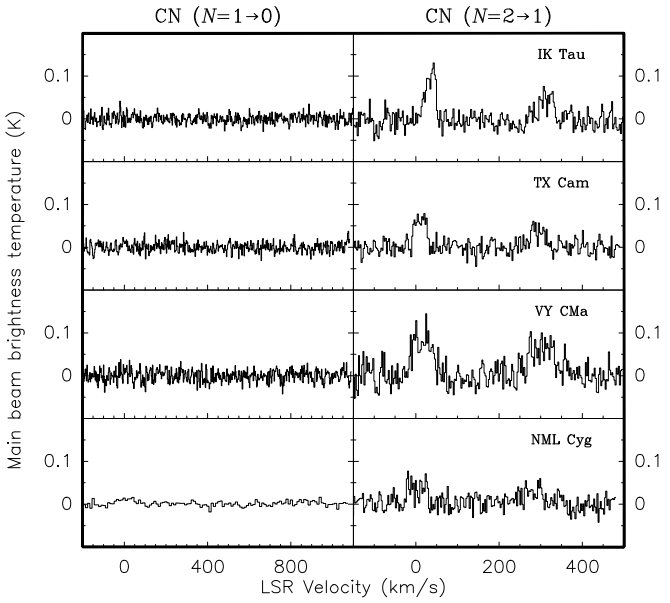

Fig. 2. CN profiles observed toward the O-rich stars with a positive detection in the N=2–1 line. The velocity scales are calculated as in Fig. 1.

HF component, (iii) the product $X = \tau(T_{\rm ex} - T_{\rm bg})$ where $T_{\rm ex}$ is the line excitation temperature that is supposed to be the same for all the fine and hyperfine components and $T_{\rm bg}$ is the background temperature, and (iv) the opacity of the main hyperfine component, $\tau_{\rm mc}$. This choice of parameters has the interesting property that when the line is optically thin, the spectrum is independent of $\tau_{\rm mc}$, that can be fixed to some arbitrary low value. The same method has been successfully used to analyze NH_3 data of interstellar clouds (e.g. Bachiller et al. 1987). In this way, we estimate that the main component opacities needed to minimize the anomalies in the observed profiles (low values of $R(1-0)$ and $R(2-1)$) are in the range 0.2 to 3.

These results are highly surprising, since even the weakest emitters, and many objects with thin envelopes (low mass loss rates) present high apparent opacities (resulting from their low R-values). It is unlikely that such envelopes are optically thick, and the present observations are better understood if the CN excitation is anomalous. In fact, an anomalous CN excitation is not unexpected in CSEs, since near-IR and visible pumping can in principle be very important in this kind of objects. In the next Section we study the rotational excitation of the CN molecule, and we describe the results of radiative transfer simulations.

4. CN excitation

4.1. Rotation temperatures

The rotation temperature, $T_{\rm rot}$, between the N=1 and 2 levels of CN can be estimated by comparing the integrated intensities of the N=1–0 and 2–1 lines. Due to the possible HF anomalies in the excitation, we assume that the lines are optically thin,

but we have checked that the rotation temperatures are not significantly changed in the case where the lines are moderately thick, i.e. if the average opacity is $\lesssim 2$ over the line profile. The resulting rotation temperatures are reported in Table 3. We have obtained typical values of $T_{\rm rot}$ in the range 3– 6 K in most C-rich envelopes. In the case of the O-rich CSEs, the non-detection of the N=1–0 line imposes lower limits to the excitation temperatures which are significantly higher than in the C-rich objects. For instance, we find $T_{\rm rot} \geq 10$ K in TX Cam, and ≥ 20 K in IK Tau and VY CMa.

4.2. CN v=0 J=2→1 masers ?

Some particular sources present a very high value of the 2–1/1–0 intensity ratio. The carbon star W Ori presents moderate intensity in the 2–1 line ($T_{\rm peak} \sim 0.5$ K), whereas the 1–0 line remains undetected at low noise levels (rms = 21 mK, see Fig. 1). A similar situation is observed in UU Aur, where the observed 2–1/1–0 ratio leads to a negative value of $T_{\rm rot}$. Such unusual values indicate that the CN v=0 J=2 level is over-thermally populated with respect to the J=1,0 levels, and suggest that some radiative pumping mechanisms are affecting the excitation. CN has important vibronic and vibrational transitions falling in the optical and in the near infrared. Pumping through such transitions could generate over-excitation in some particular v=0 rotational levels and produce weak masers as that observed in the CN 2–1 line towards UU Aur.

It is worth noting that these two objects are known to present anomalous HCN v=0, J=1–0 emission: their HCN profiles are spiky and display strong variability (Olofsson et al. 1993b ; Izumiura et al. 1995). The ground-state HCN 1–0 line emission in these objects is thus of maser nature. From the 6 other stars known to present HCN masers, Y CVn, RY Dra, TU Gem, X Vel, X TrA and Y Tau, we only observed the two first in the CN lines. However, the relative CN 1–0 and 2–1 intensities of these objects do not suggest significant effects of maser action in CN. It thus appears that the possible maser action in the ground-state of CN is less dramatic than that of HCN v=0.

4.3. LVG transfer calculations

In order to check the validity of the $T_{\rm rot}$ values derived from the 2–1/1–0 intensity ratio, we have carried out numerical simulations of the radiative transfer with a Large-Velocity-Gradient (LVG) code. The fine structure components are assumed to present no line overlap. On the other hand, the hyperfine components are considered as being completely coincident. This is well justified for high rotational transitions, but it is less obvious for the two lowest lines. In any case, our calculations show that these two low-J transitions are the ones that present the lowest opacity, so line overlap is expected to be unimportant since it has no effect in the optically thin limit. We assumed that the molecules are excited through the IR v=1–0 transition near 4.8 μm, as well as by collisional excitation. The collisional rates of CN are unknown, so we used those of CS (Green & Chapman 1978) corrected for the different molecular sizes, and

Table 3. Estimated CN fractional abundances

Source	$T_{\rm rot}$ (K)	r_i (cm)	r_e (cm)	$X_{\rm CN}$
C-rich objects:				
IRC+60041	9	1.8(15)	1.9(16)	1.0(−5)
AFGL 190	6[a]	1.9(16)	5.4(16)	≤1.2(−6)
AFGL 341	6[a]	1.3(16)	3.7(16)	≤1.2(−6)
U Cam	5	1.6(15)	1.6(16)	5.8(−5)
IRC+60144	5	2.8(15)	1.8(16)	6.6(−6)
W Ori	≥53[b]	8.1(14)	8.6(15)	2.7(−5)
AFGL 809	6[a]	8.8(15)	4.1(16)	≤7.2(−7)
UU Aur	≤−75[b]	1.4(15)	1.2(16)	9.8(−6)
CL Mon	6	1.6(15)	2.0(16)	1.1(−5)
AFGL 5254	6[a]	3.8(15)	1.8(16)	≤4.5(−7)
IRC+10216	6	1.0(16)	3.3(16)	6.2(−7)
CIT-6	4	4.8(15)	2.3(16)	8.3(−6)
VY UMa	6[a]	6.9(14)	6.6(15)	≤1.2(−5)
V Hya	6	2.0(15)	1.7(16)	3.1(−6)
Y CVn	5	6.9(14)	6.7(15)	7.9(−5)
RU Vir	5	2.7(15)	1.8(16)	1.1(−5)
RY Dra	6	9.5(14)	9.2(15)	5.1(−5)
V CrB	6[a]	1.0(15)	7.4(15)	≤5.0(−6)
T Dra	8	1.5(15)	1.2(16)	2.3(−6)
IRC+20370	3	3.0(15)	1.7(16)	7.4(−6)
V Aql	6[a]	6.7(14)	7.4(15)	1.7(−5)
AFGL 2494	6[a]	7.9(15)	3.4(16)	≤2.2(−7)
V Cyg	5	1.9(15)	1.3(16)	8.6(−6)
S Cep	5	1.7(15)	2.0(16)	2.1(−5)
AFGL 3068	4	1.5(16)	4.2(16)	2.0(−6)
LP And	5	5.0(15)	2.2(16)	4.3(−6)
O-rich objects:				
IRC+10011	20[a]	6.0(15)	2.9(16)	≤1.9(−7)
IK Tau	≥ 20[c]	3.4(15)	2.1(16)	6.8(−8)
TX Cam	≥ 10[c]	2.5(15)	1.7(16)	1.1(−7)
α ORI	20[a]	1.0(15)	1.1(16)	≤ 2.4(−7)
VY CMa	≥ 25[d]	2.9(16)	8.9(16)	4.6(−8)
OH26.5+0.6	20[a]	3.5(16)	7.0(16)	≤ 3.0(−8)
NML Cyg	20[a]	8.4(15)	3.8(16)	3.9(−8)
Other objects:				
AFGL 618	6	1.0(17)	1.7(17)	2.1(−6)
OH231.8+4.2	6[a]	2.2(17)	3.3(17)	≤ 1.1(−8)
S Sct	6[a]	1.2(15)	1.4(16)	≤ 3.1(−7)
W Aql	5	3.3(15)	2.0(16)	1.2(−5)
IRC+10420	7	3.1(16)	1.1(17)	4.7(−7)
χ Cyg	16	6.8(14)	7.0(15)	8.6(−7)
AFGL 2688	4	2.2(17)	3.2(17)	1.0(−6)
NGC 7027	3	1.3(17)	2.0(17)	2.3(−7)
SAO 96709	6[a]	1.3(16)	3.6(16)	2.2(−6)

[a] Assumed value due to lack of data.
[b] $T_{\rm rot}$ = 6 K assumed in the abundance estimate due to anomalous rotational excitation.
[c] $T_{\rm rot}$ = 20 K assumed in the abundance estimate.
[d] $T_{\rm rot}$ = 25 K assumed in the abundance estimate.

we assumed the infinite order sudden (IOS) approximation to account for the fine structure. Although such rates are clearly inadequate to study details of the CN collisional excitation, they should be approximate enough for the estimates of the rotation temperatures. The values assumed for the mass loss rate $\dot{M}$, the expansion velocity, V_e, and the stellar emission near 4.8 μm are taken within the usual ranges in CSEs (see e.g. Table 1). A standard kinetic temperature profile was assumed for the envelope (e.g. Kwan & Linke 1982); in the region relevant to the CN emission, T_K varies from about 40 to 15 K. The abundance of CN was assumed to be in the range 10^{-7} – 10^{-5} and constant in the emitting region (see below).

The aim of this model is not to explain each star individually but to figure out the physical processes that determine the trends observed in the CN excitation. We find that under the physical conditions discussed here (in particular, provided that the rotational lines are not very optically thick), the excitation of the lowest levels is mainly radiative, so it is not very sensitive to the CN collisional rates and to other parameters dependent on the individual stars such as the fractional abundance of CN, X_{CN}, $\dot{M}$, T_K and V_e. We obtain that the rotation temperature decreases significantly with the distance to the star. T_{rot} = 4– 7 K at a typical distance from the star of about 4 10^{16} cm. Typical values of T_{rot} = 15– 20 K are found in a narrow region around a radius of 2 10^{16} cm. However, T_{rot} increases quickly in this region, and the population becomes inverted at slightly smaller distances to the star.

If CN is the direct photodissociation product of HCN, the CN molecules are expected to be concentrated in a shell external to the HCN region (see below). This CN shell will be closer to the star in a small envelope than in a more extended CSE. As a consequence, our calculations predict that the CN molecules in small envelopes will present higher excitation than in more extended CSEs. Moreover the anomalously high rotational excitation and masers are expected to happen in small objects preferably. These calculations also suggest that the differences found between the excitation of C-rich and O-rich objects could be due to differences in the envelope size, and consequently in the distance of the emitting region to the star. In such a case, the average radii of the CN shells in O-rich envelopes would be about a factor of 2 smaller than in C-rich objects.

Giving the simplicity of our model, it is not surprising that it does not account for the observed anomalous R ratios (see previous section). In particular, our treatment of the component overlap is crude, probably affecting the reliability of the component ratio predictions.

We finally stress that the effect of the excited low-lying $^2\Pi$ electronic state is unknown, and deserves further investigation. The transitions from this state (the CN "red band") are near 1.1 μm, and are known to be very bright in many stars. It seems plausible that pumping through this electronic state could dominate to the pure vibrational pumping in the objects which are bright around 1 μm. The study of such excitation mechanism would require a non-local treatment of the radiative transfer, since the envelopes are expected to be very optically thick near 1 μm. Such detailed models are out of the scope of the present work, but we consider very likely that pumping through the $^2\Pi$ state could explain the anomalies in the CN excitation reported here, in particular the departures of the R ratios from the LTE values.

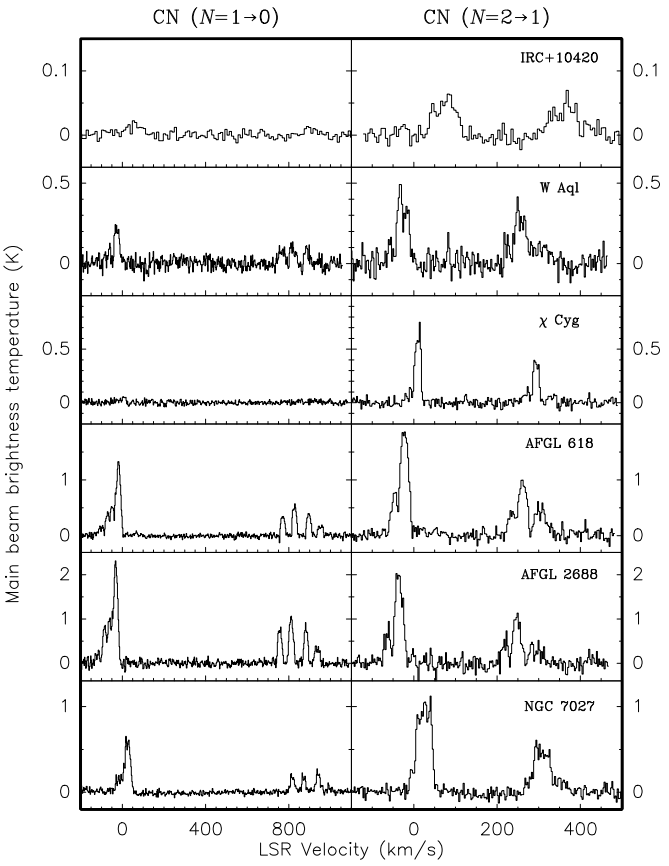

Fig. 3. CN profiles observed toward selected miscellaneous objects (see also Table 1). The velocity scales are calculated as in Fig. 1.

5. The abundance of CN in circumstellar envelopes

5.1. CN as a result of the photodissociation of HCN

Chemical models predict that in carbon stars CN is formed from the photodissociation of HCN (Huggins & Glassgold 1982, Lafont et al. 1982, Huggins et al. 1984, Nejad & Millar 1987, Truong-Bach et al. 1987, Cherchneff et al. 1993, Millar & Herbst 1994). CN is produced in a shell, surrounding the HCN envelope, in which the ambient ultraviolet radiation is able to penetrate to convert the HCN into CN. We are going to show in this section that, in spite of the large uncertainties involved in both the empirical and theoretical abundance determination, the model predictions are compatible with our observational results.

The study of the CN/HCN ratio seems the best way to set constraints to the mechanisms of formation of CN. If CN is formed from the HCN photodissociation, the HCN molecules will preferably reside in an inner region surrounded by a shell of CN. Such configuration will have implications on the relative *total* number of molecules for CN and HCN. In progressively

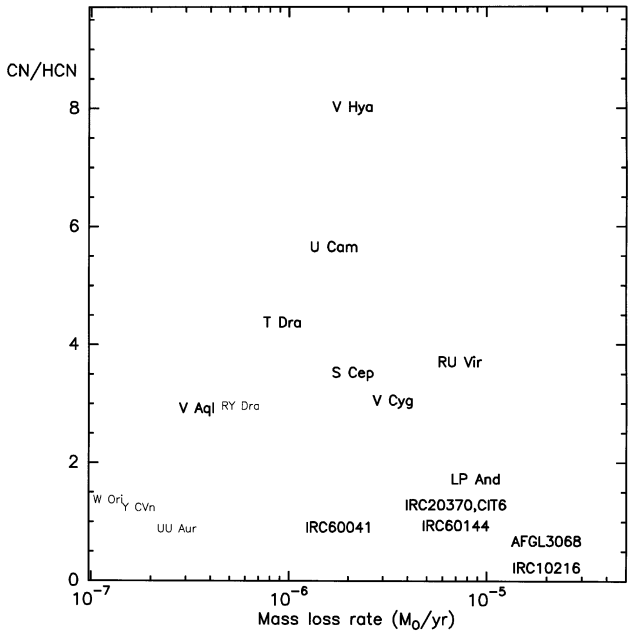

Fig. 4. CN(2–1)/HCN(1–0) line intensity ratio versus the mass-loss rates for C-rich stars. The objects marked with smaller symbols are HCN v=0 J=1–0 masers. Anomalous rotational excitation in the CN lines is observed in W Ori and UU Aur (see discussion in the text).

thicker envelopes, the total number of HCN molecules will increase accordingly, but the total number of CN molecules is not expected to increase in the same way since the depth of the CN shell should remain nearly constant. Thus the CN/HCN total number ratio is expected to decrease for objects with increasing mass loss rates.

In first approximation (assuming in particular optically thin emission, and that the excitation conditions do not vary a lot from object to object), the ratio of the total number of CN and of HCN molecules should be proportional to the ratio of the velocity integrated intensities. We have plotted in Fig. 4 this intensity ratio for the CN(2–1) and HCN(1–0) lines versus the mass-loss rates taken for C-rich stars. The points in this plot present a relatively high scatter, in part because some effects such as the line opacities are not taken into account. In particular, the HCN(1–0) line is expected to be optically thick in many C-rich stars. For such stars, the ratio of the integrated intensities of the CN(2–1) and HCN(1–0) lines would only provide an upper limit to the ratio of the total number of molecules. However, the advantage of the plot in Fig. 4 is that it is fully observational, i.e. it does not contain any model-dependent assumption. In spite of the large scatter, some systematic trend can be perceived in this plot. The highest values of the CN/HCN ratio are found in objects with low to moderate envelope thickness ($\dot{M} \leq 3\ 10^{-6}$), while the lowest CN/HCN ratios are found in thick envelopes ($\dot{M} > 3\ 10^{-6}$).

There are three objects (W Ori, UU Aur, and Y CVn), which seem to behave in a peculiar way. These are thin envelopes in which the CN/HCN intensity ratio is close to unity, instead of the values 3– 8 which seem to be the rule in thin envelopes. However, such low values do not seem to be due to chemical effects. In fact, as discussed above, these three objects (and RY Dra) are known to present anomalous HCN v=0, J=1–0 emission. (Olofsson et al. 1993b ; Izumiura et al. 1995). The HCN line emission in these objects is probably of maser nature, leading therefore to anomalously intense emission. In two of these objects (UU Aur and W Ori) the CN excitation measured from the 2–1/1–0 line ratio is anomalously high. To summarize, the CN/HCN line intensity ratio in these three sources cannot be considered as a relative measurement of the ratio of total number of molecules, since the CN/HCN intensity ratio is distorted by maser effects. In addition, we note that Y CVn is a J-star known to present important abundance anomalies.

We thus conclude that, generally speaking, the CN/HCN abundance ratio in carbon stars decreases as the envelope thickness increases. We further note that the opacity effects in the HCN line would tend to mitigate this observed trend (Fig. 4), since they should mask the larger number of HCN molecules in the heavier envelopes. The fact that this trend is still seen in Fig. 4, in spite of the probably high HCN opacity in objects with mass loss rates as high as 10^{-5} $M_{\odot}yr^{-1}$, strongly suggests that this relation actually holds in C-rich circumstellar envelopes. As quoted above, this is the expected behavior if CN is formed from the photodissociation of HCN.

5.2. The size of the CN emitting region

One of the most critical parameters in estimating the CN abundance in CSEs is the size of the CN emitting region. By doing strip-maps we measured the envelope sizes in two carbon objects, IRC+10216 and CIT 6, and found a radius of $5\ 10^{16}$ and $4\ 10^{16}$ cm, respectively. The angular resolution of these observations was not high enough to resolve the shell structure of the CN emitting region. However, recent interferometric observations of the CN N=1–0 line in IRC+10216 (Lucas et al. 1995; Dayal & Bieging 1995) confirm that the emission comes from a relatively thin shell of radius about $6\ 10^{16}$ cm. The observed morphology and the measured radii are consistent with the models in which CN is the main product from the HCN photodissociation. The external radius of the CN emitting shell predicted by the models is about 2– 3 times larger than the HCN region (e.g. Huggins et al. 1984, Truong-Bach et al. 1987).

No measurements of the CN envelope sizes are available in O-rich stars. However, the HCN emitting region has been measured at the IRAM interferometer (Fuente & Guilloteau, private communication) to be typically $\sim\ 10^{16}$ cm in a sample of O-rich objects. Thus, the HCN envelopes of the O-rich stars appear to be 2– 3 times smaller than those of the carbon stars, and it seems plausible that the CN envelopes behave in a similar way. This suggest that the CN envelopes of O-rich stars have typical radii of about $2\ 10^{16}$ cm, in agreement with the higher CN excitation observed in the O-rich objects ($T_{\rm rot} \geq$ 10– 20 K, to be compared with the 3– 6 K found in carbon CSEs).

With the exception of IRC+10216 and CIT 6, no measurements of the sizes of the CN emitting regions in CSEs are available so far. In order to estimate the spatial extent of the CN

emitting regions in the objects of our sample, we have assumed that the photodissociation of HCN is the only mechanism of CN production. This is supported, for C-rich stars, by the behavior of the CN/HCN ratio studied in Section 5.1. We have also assumed than CN is only destroyed by photodissociation, and we have only considered the shielding by dust. The inner and outer radii of the CN shells are thus fixed by the photodissociation processes, and can be estimated with the procedure described by Huggins & Glassgold (1982) and Olofsson et al. (1993b). We have used the photodissociation rates for CN and HCN given by van Dishoeck (1988). The parameter $\dot{M}_d/v_d$ (i.e. the dust mass-loss rate divided by the dust expansion velocity), which determines the dust shielding distance (see Jura & Morris 1981), has been estimated from the IRAS fluxes at 60 μm by assuming the distances listed in Table 1 and the luminosities quoted in Loup et al. (1993). For some stars (NML Cyg, AFGL2688, NGC7027, and OH231.8+4.2) we used the parameters given by Sopka et al. (1985). In the case of IRC+10420, we considered the luminosity given by Oudmaijer (1995). The resulting radii are given in Table 3, and are in very good agreement with the estimates of Olofsson et al. (1993b) for the common objects.

This model is unsuited for objects with bipolar morphology as the proto-PNe, and for detached envelopes. For instance, Lindqvist et al. (1996) report a radius of $7\,10^{16}$ cm for the external envelope of U Cam, i.e. $\sim$3 times larger than the value given in Table 3. On the other hand, the model assumes that photodissociation processes are the only mechanisms of formation and destruction of CN in both C-rich and O-rich objects. This assumption is unsuited for O-rich stars (Nejad & Millar 1988, Nercessian et al. 1989). In fact, interferometric observations (Fuente & Guilloteau, private communication) and the study of the CN excitation (Section 4.3) suggest that the CN shells are smaller within O-rich objects than within C-rich CSEs. As we will discuss below, it appears that CN in O-rich stars is destroyed by additional mechanisms than photodissociation. Then, the simple model used here to estimate the shell radii could not be well suited to O-rich objects, and the reported radii would be overestimated for this kind of stars. Nevertheless, for homogeneity, we have estimated the CN abundances for all stars with the radii of Table 3.

5.3. CN abundances

In order to estimate the abundance of CN in the program objects, we followed the method described in Ukita & Morris (1983) (see also Bujarrabal et al. 1994), that assumes optically thin emission. We considered that the fractional abundance and the excitation are constant in the CN shells. We assumed that the excitation of the full rotational ladder is determined by $T_{\rm rot}$, as calculated from the 2–1/1–0 ratio listed in Table 3 (see Section 4.1). Distances, expansion velocities, and mass loss rates were taken from Table 1. The obtained CN abundances are listed in Table 3. For the stars W Ori and UU Aur which present anomalous excitation in the N=2, 1 levels, we used a representative excitation temperature of 6 K, similar to that found in other carbon CSEs.

Table 4. Comparison of CN and HCN peak abundances derived from observations and models

		$X_{\rm CN}$	$X_{\rm HCN}$	$X_{\rm CN}/X_{\rm HCN}$
C-rich	observed[a]	1.9(−5)	4.2(−5)	0.45
	models[b]	∼8(−6)	∼5(−6)	0.6
O-rich	observed[a]	6.6(−8)	1.6(−6)	0.04
	models[c]	4-40(−8)	∼4(−8)	1-10

Notes.- [a] Average values for the stars detected in CN. [b] e.g. Millar & Herbst (1994). [c] Nejad & Millar (1988), Nercessian et al. (1989)

The CN abundances range from a few 10^{-7} up to 10^{-5} in carbon stars. The average abundance in the detected carbon objects is $1.9\,10^{-5}$. These figures are in general agreement with the results of Olofsson et al. (1993b), and with chemical models (e.g. Nejad & Millar 1987, Cherchneff et al. 1993). A comparison of the abundances derived from observations and models is given in Table 4. We also list the CN/HCN peak abundance ratios. The observational HCN abundances have been estimated from data of Bujarrabal et al. (1994). For C-rich stars we have used the sizes determined from the photodissociation theory (we have considered that the radius of the HCN emission region is the internal radius of the CN shell). We obtain an average value CN/HCN $\sim$0.45, to be compared with the values in the range 0.58 to 0.65 predicted by the photodissociation model. Observations and theory seem to be in good agreement for carbon stars. However, we would like to point out that the HCN abundances are usually derived by assuming optically thin emission. Indeed more accurate estimates taking into account the HCN opacities would be desirable.

Out of the five O-rich stars detected in CN, two are AGB stars, two are red supergiants and the last one is IRC+10420, a peculiar object whose the evolutive stage is unclear. In O-rich AGB stars and red supergiants, the CN abundance ranges from $\lesssim 3\,10^{-8}$ to 10^{-7}, and the average CN abundance is $\sim 6.6\,10^{-8}$. These values are of the same order than that reported for TX Cam by Olofsson et al. (1991). For IRC+10420 we report a larger CN relative abundance of $3\,10^{-7}$, but we note that it is not clear that our simple model can be applied to this peculiar object. In particular, its enormous mass loss rate could imply that the radius for the emitting region is unusually large, which could explain the intense emission without invoking a so large CN abundance. The CN abundance predicted by the models for O-rich stars is (4–40) 10^{-8}, so the observed value is close to the lowest of the model predictions.

To estimate the HCN abundances in O-rich stars, we have considered that HCN resides in a shell whose external radius is half that of CN, as suggested by chemical models (Nercessian et al. 1989). For the oxygen stars detected in CN, the average HCN abundance is $\sim$40 times higher than the value predicted by models (see Table 4).

The average CN/HCN peak abundance ratio is 0.04 in O-rich stars, whereas chemical models predict a value in the range 1 to 10 in this kind of objects (Nejad & Millar 1988; Nercessian et al. 1989). We thus conclude that in O-rich stars CN is destroyed by additional mechanisms than photodissociation. In fact, Olofsson et al. (1991) have previously suggested that, in O-rich CSEs, CN could be efficiently destroyed by reacting with atomic oxygen, CN + O —> CO + N. The possibility that CN is destroyed by such mechanisms casts doubts on the radii listed in Table 1 for oxygen stars, since these radii were derived by assuming that CN is only destroyed by photodissociation, and seems to confirm that O-rich CSEs are smaller than C-rich stars (as indicated by observations and the excitation considerations mentioned above). We note that assuming a smaller size for oxygen stars will produce a correspondingly higher CN abundance. Still, if the CN radii are of the order of $2\,10^{16}$ cm (see Sect. 5.2), substantial CN/HCN differences remain between observations and theory for O-rich stars: the observed CN/HCN ratio is about two orders of magnitude smaller than the value predicted by models.

The HCN and CN peak abundances are about 20 and 300 times higher, respectively, in C-rich stars than in O-rich objects. These differences can not be attributed to opacity effects, since it is also observed for the optically thin carbon objects. It is interesting to note that HCN seems particularly abundant just in the O-rich sources in which CN has been detected. In other O-rich stars the HCN abundance is in the average ~ 4– $10\,10^{-7}$ (Bujarrabal et al. 1994). The high HCN abundance found in O-rich stars is not yet understood, since chemical models predict abundances at most 10 times smaller than the measured values (e.g. Nejad & Millar 1988). On the other hand, the HCN v=0 J=1–0 is known to present anomalous excitation in some optically thin carbon envelopes, but the importance of such effects in oxygen stars remains unknown. A careful analysis of the HCN excitation is this kind of sources is necessary, since weak masers in the v=0 J=1–0 line could result in an over-estimate of the abundances derived from observations.

6. Conclusions

We have carried out a survey of CN N=1–0 and N=2–1 line emission in circumstellar envelopes around evolved stars. Our sample includes C- and O-rich stars, S-type stars, and protoplanetary nebulae. The main conclusions of this work are:

1.– Confident detections are reported for 30 sources, including 5 O-rich stars. It is to be noted that previously to this work, CN had been only detected in one O-rich evolved star (TX Cam, Olofsson et al. 1991).

2.– The excitation temperature derived from the 2–1/1–0 intensity ratio is relatively low in C-rich stars, of the order of 3–6 K. In O-rich stars the excitation temperature is in excess of 10–20 K. LVG calculations show that this CN excitation is expected for typical distances of the order of $4\,10^{16}$ and $2\,10^{16}$ cm. Thus, CN shells in O-rich envelopes could be closer to the star than in C-rich sources, in agreement with the scarce existing measurements of the CN and HCN extents.

3.– Rotational anomalies are observed in the form of unusual high values of the 2–1/1–0 intensity ratios in two carbon objects, W Ori and UU Aur, which are also known to present anomalous (presumably maser) HCN excitation in the v=0 state. Pumping through the optical and near-IR CN bands seems the most likely mechanism to over-populate some particular rotational levels of CN. UU Aur seems to present weak maser action in the 2–1 line.

4.– Fine and hyperfine excitation anomalies are seen in C– and O-rich stars: the relative intensities of the fine and hyperfine components are different from the relative line strengths. At first sight, one could think that these anomalies are due to high opacities. However, this would require excessively high opacities. We find particularly surprising that the strongest anomalies are observed in the sources with the lowest mass-loss rates. We propose that excitation effects play a dominant role in this phenomenon.

5.– In carbon stars CN is expected to be formed from photodissociation of HCN. In order to further check this idea, we have compared the velocity integrated intensity of CN N=2–1 with that of the HCN J=1–0 line in C-rich stars. In optically thin CSEs, this ratio is expected to be proportional to the ratio of total number of molecules. Except for three stars that are known to present anomalies in the HCN and CN emissions, the line ratio is clearly observed to decrease at increasingly mass loss rates. It is noteworthy that the effects of the probably high opacity of the HCN line would tend to destroy the observed trend. We thus conclude that our data provide support to the formation of CN from photodissociation of HCN in carbon stars.

6.– We have estimated the radii of the CN shells from the properties of the envelopes and the CN and HCN photodissociation rates. We have then computed the CN abundances in the optically thin case, assuming the excitation temperatures obtained from the line ratios. The CN abundances range from a few 10^{-7} up to 10^{-5} in carbon stars, and from $\lesssim 3\,10^{-8}$ to 10^{-7} in O-rich objects. It thus appears that CN is about two orders of magnitude less abundant in O-rich stars than in C-rich stars.

7.– The CN/HCN peak abundance ratio is $\sim$0.45 in C-rich stars in agreement with chemical models. This ratio is $\sim$0.04 in O-rich objects, a factor in the range 25– 250 smaller than the value predicted by available models. Such models predict an excessively high CN abundance, and are deficient in HCN by about two orders of magnitude. Some additional mechanisms for the destruction of CN in O-rich objects, such as the reaction of CN with atomic oxygen, could solve the CN problem, but the high observed HCN abundances would remain unexplained.

Acknowledgements. This work has been partially supported by Spanish DGICYT grant PB93-048.

References

Bachiller R, Guilloteau S, Kahane C. 1987. A&A 173, 324

Bachiller R, Forveille T, Huggins PJ, Cox P. 1996, in preparation
Bujarrabal V, Cernicharo J. 1994. A&A 288, 551
Bujarrabal V, Fuente A, Omont A. 1994. A&A 285, 247
Cherchneff I, Glassgold AE, Mamon GA. 1993. ApJ 410, 188
Cox P, Omont A, Huggins PJ, Bachiller R, Forveille T. 1993. A&A 266, 420
Dayal A, Bieging JH. 1995. ApJ 439, 996
Green S, Chapman S. 1978. ApJS 37, 169
Huggins PJ, Glassgold AE. 1982. ApJ 252, 201
Huggins PJ, Glassgold AE, Morris M. 1984. ApJ 279, 284
Izumiura H, Ukita N, Tsuji T. 1995. ApJ 440, 728
Jura M, Morris M. 1981. ApJ 251, 181
Kwan J, Linke RA. 1982. ApJ 254, 587
Lafont S, Lucas R, Omont A. 1982. A&A 106, 201
Lindqvist M, Lucas R, Olofsson H, Omont A, Eriksson K, Gustafsson B. 1996. A&A 305, L57
Loup C, Forveille T, Omont A, Paul JF. 1993. A&ASS 99, 291
Lucas R, Guélin M, Kahane C, Audinos P, Cernicharo J. 1995. A&Space Sci 224, 293
Nejad LAM, Millar TJ. 1987. A&A 183, 279
Nejad LAM, Millar TJ. 1988. MNRAS 230, 79
Millar TJ, Herbst E. 1994. A&A 288, 561
Nercessian E, Guilloteau S, Omont A, Benayoun JJ. 1989. A&A 210, 225
Olofsson H, Lindqvist M, Nyman L-A, Winnberg A, Nguyen-Q-Rieu. 1991. A&A 245, 611
Olofsson H, Eriksson K, Gustafsson B, et al. 1993a. ApJS 87, 267
Olofsson H, Eriksson K, Gustafsson B, et al. 1993b. ApJS 87, 305
Omont A. 1985, in "Mass loss from red giants", Ed. M. Morris & B. Zuckerman, Dordrecht: Reidel, p. 269
Omont A. 1992, in "Faraday Symp. 28: Chemistry in the interstellar medium".
Omont et al. 1993, quoted in Loup et al. (1993)
Oudmaijer RD. 1995. Ph. D. Rijksuniversiteit Groningen
Sopka RJ, Hildebrand R, Jaffe DT, Gatley I, Roellig T, Werner M, Jura M, Zuckerman B. 1995. ApJ 294, 242
Truong-Bach, Nguyen-Q-Rieu, Omont A, Olofsson H, Johansson LEB. 1987. A&A 176, 285
Ukita N, Morris M. 1983. A&A 121, 15
van Dishoeck EF. 1988, in "Rate Coefficients in Astrochemistry", eds.: TJ Millar & DA Williams. Dordrecht: Kluwer.

This article was processed by the author using Springer-Verlag LaTeX A&A style file *L-AA* version 3.